A Coordinated Multi-Element Current Differential Protection Scheme for Active Distribution Systems

Vassilis C. Nikolaidis, *Senior Member, IEEE,* George Michaloudis, Aristotelis M. Tsimtsios, *Member, IEEE,* Dimitrios Tzelepis, *Member, IEEE,* Campbell D. Booth

***Abstract*--This paper introduces a current differential protection scheme, appropriate for application in medium voltage active distribution systems, where it is desired to keep the greatest possible number of loads and DG units energized during a fault. Conventional two-terminal percentage current differential relays are used to form successive, time-current-coordinated, differential protection zones. Multiple time-delayed differential elements in each protection zone guarantee coordination with the zone's lateral protection devices, as well as between successive differential protection zones. Sensitive time-delayed differential elements protect against relatively high-resistance faults, while instantaneous differential elements minimize protection speed whenever possible. Additional emergency differential elements deal with post-fault topology changes and breaker failure conditions enhancing the overall scheme's performance. The proposed scheme is applied to a model of real medium voltage distribution system with distributed generation, considering a ring topology operation. A detailed simulation-based study proves the applicability and enhanced performance of the proposed scheme.**

***Index Terms*--Differential protection, distributed generation, percentage differential relay, power distribution systems, protection coordination.**

I. Introduction

THE prospect of mass integration of distributed generation (DG) into distribution systems requires, among others, the design of new protection schemes, given the unsuitability of conventional overcurrent protection under these conditions [1]. Most of the relevant proposed protection solutions utilize directional overcurrent protection schemes, based on optimization algorithms [2], [3], adaptive logic [4], [5], or pilot-based logic [6], [7]. A basic limitation of such solutions is that coordination with existing lateral protection means is not addressed. Other research efforts follow alternative protection approaches, e.g., employing deep neural networks, dynamic state estimation, or a multifunctional logic [8]-[10]. However, the applicability of these approaches with commercial relays cannot be considered immediate since they rely on advanced infrastructure and network awareness.

Since the operation conditions of modern/future distribution systems with DG (i.e. bidirectional short-circuit current flow and/or closed-loop configuration) resemble those of transmission systems, protection principles traditionally encountered in the latter, have been also considered for the former. Within this context, distance-based protection schemes have been proposed for DG-integrated distribution systems [11]-[13]. Nevertheless, a drawback of such schemes is the requirement for a voltage transformer, along with each relay.

On the other hand, line current differential protection has been envisioned as a promising solution for radial or closed-loop DG-integrated distribution systems over the last years. Current differential protection schemes for radial distribution systems with DG have been proposed in [14]-[23]. A limitation of [14]-[20] is that the effect of intermediate DG infeed or load on differential protection performance is not addressed. The DG infeed effect is especially critical in terms of false tripping, not only during normal system operation, but also during external faults, which may require coordination between successive differential relays (DRs). In [21], the differential protection scheme is properly set to prevent erroneous tripping due to intermediate loads, without, however, examining coordination with the protection means of the respective laterals, or the effect of intermediate DG.

Inverter-interfaced DG (IIDG) units are considered inside differential protection zones (DPZs) in [22], [23], where a methodology for estimating the short-circuit contribution of intermediate IIDG units is proposed. However, the effect of intermediate loads and coordination with lateral protection are not addressed. The effect of intermediate DG infeed is taken into account in [24], but only for low-infeed IIDG units; hence DR coordination issues during external faults do not arise.

The increased reliability requirements of closed-loop distribution systems with DG have rendered differential protection a good match for such applications [25]-[29]. In this case as well, a basic limitation of the proposed schemes is that neither coordination with lateral protection, nor the effect of intermediate DG infeed or load is addressed. The differential protection scheme proposed in [30] is properly set to prevent erroneous tripping due to intermediate load outfeeds, as well as to coordinate with lateral protection; in fact, an inverse time-differential-current characteristic is applied for the latter purpose. However, besides not complying with the capabilities of

V. C. Nikolaidis and G. Michaloudis are with the Department of Electrical and Computer Engineering, Democritus University of Thrace (DUTH), Xanthi, Greece (e-mails: vnikolai@ee.duth.gr; geormich21@ee.duth.gr).

A. M. Tsimtsios is with PROTASIS SA, 59B Apostolopoulou Street 15231 Chalandri, Athens, Greece (e-mail: atsimtsios@protasis.net.gr).

D. Tzelepis and C. D. Booth are with the Department of Electronic and Electrical Engineering, Strathclyde University, Glasgow, United Kingdom (e-mail: dimitrios.tzelepis@strath.ac.uk; campbell.d.booth@strath.ac.uk).

most commercial DRs, coordinating such a characteristic with a typical inverse time-current characteristic is challenging, as each characteristic refers to a different type of measured current. Moreover, intermediate DG units are not considered in this work either.

A preliminary differential-based protection solution against the limitations of existing relevant studies has been proposed by the authors in [31]. However, in this work, a single main differential element is enabled in each DPZ, which does not permit a concurrently selective and fast DR operation.

This paper reconsiders the above practice, proposing a multi-element differential protection scheme for active distribution systems, where it is desired to disconnect the smallest possible network part during faults (to avoid mass load/DG disconnection or potentially sustain an intentional island). The main contributions of this work are the following:

- A new differential protection approach is introduced, where each relay uses multiple time-graded current differential elements for primary protection, ensuring at the same time coordination with lateral protection and fast enough operation during main line faults.
- The complimentary use of multiple elements in each DR provides adequate protection speed and selectivity under both normal and post fault distribution system topology, thus increasing protection and distribution system operation reliability to the greatest extent possible.
- The proposed relay setting methodology compensates for the effect of intermediate load and DG, preventing erroneous tripping during normal operation and external faults. To address the latter case, instead of desensitizing DRs, a time-graded coordination approach is followed.
- The proposed protection scheme is based on existing DR capabilities and simple current differential characteristics, commonly encountered in commercial relays. This enhances the applicability of the presented solution.

The rest of this paper is organized as follows. Section II introduces the basic principle of the proposed differential protection scheme. Section III describes the normal setting procedure of the differential elements, whereas Section IV addresses the same procedure considering emergency conditions in the distribution system. Section V summarizes the main findings from the application of the proposed protection scheme in a replica of an actual distribution system, whereas Section VI concludes the paper.

II. Introducing the Proposed Current Differential Protection Concept

Let us consider a section of an illustrative medium voltage (MV) power distribution feeder with DG (Fig. 1). Protection devices (PDs) are assumed to be installed along each lateral and up to the primary of MV / low voltage (LV) power distribution transformers. For simplicity, only the remotest MV/LV power distribution transformer at each lateral is shown in Fig. 1, whereas lateral loads have been concentrated at this point.

Assume further that a numerical DR is installed at several measurement points of the main feeder line, as shown in Fig. 1. The decision on the number of DRs depends on the system operation experience, the desired system reliability level (which depends on the ability of the system to maintain the largest possible number of loads and DG units, or to partially operate in an intentionally islanded mode after a fault), and ultimately on financial issues, and is normally made by the distribution system operator. It is noted that determining the optimum number of DRs is out of the scope of this paper.

A pair of DRs forms a DPZ, covering a part of the main feeder line and the connected laterals up to the remotest MV/LV power distribution transformer (illustrated with the red dashed line). The DPZ simultaneously provides primary protection against faults occurring in the main feeder and backup protection against faults occurring in the laterals. If fuses are the lateral PDs, a fuse blowing philosophy should be adopted for the backup protection scheme. The DRs assigned to a DPZ continuously exchange current measurements received from current transformers (CTs) installed at the measurement points. For this purpose, a fast communication channel between the DRs is required.

Under normal system conditions, load currents are flowing in all circuit branches. Due to the lateral loads and the DG units connected to the main feeder in between the CTs of a DPZ, a differential current is always measured by the DRs of this zone under normal (non-fault) system conditions. Differential currents are also measured by the DRs if a short-circuit fault occurs internally or externally to a DPZ. Internal faults are those occurring in the main feeder line or in the laterals of the area covered by the DPZ of interest. External faults are those occurring in a neighbor DPZ. In the latter case, a differential current may be sensed by the DRs of the non-faulted DPZ due to the DG infeed effect.

To retain coordination between the DRs and the lateral main PDs (MPDs) of a DPZ, a time delayed trip is introduced to the DRs of this zone. Note that each lateral's MPD is supposed to be properly coordinated with all the downstream PDs. Hence, setting of downstream lateral PDs is not of interest in this work. Nevertheless, in order to increase protection security, each DPZ is set not to detect faults occurring in the LV part of the distribution system.

Besides guaranteeing coordination between the DRs of a DPZ and the lateral PDs, selectivity between the DRs of successive DPZs should also be guaranteed. Therefore, a time-current-graded coordination between successive DPZs is additionally considered.

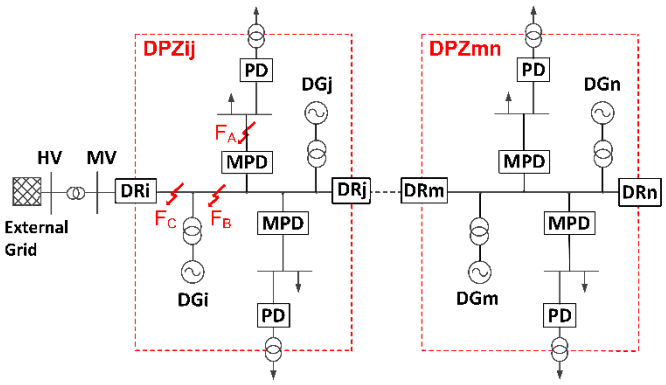

Fig. 1. DPZ formation in a typical power distribution system.

To sum up, the DRs of each DPZ must operate reliably under all the critical fault and non-fault conditions and all the possible grid operation states. Overall, DRs should be set to:

- Prevent trip during normal non-fault system conditions, irrelative of load/generation level and grid configuration.
- Clear every single fault occurring inside a DPZ, at least for a specified fault-resistance range.
- Provide a time-delayed trip command to ensure coordination with the lateral MPDs, in case of lateral faults.
- Not detect faults occurring in the LV network.
- Preserve selectivity between successive DPZs to avoid nuisance tripping (e.g. due to DG infeed effect).

III. Differential Relays Setting Philosophy

The proposed current differential protection scheme utilizes a pair of DRs to form an enhanced DPZ. Multiple differential elements of the DRs pair are enabled to protect the DPZ. The differential elements are set based on a systematic offline simulation procedure conducted once. Note that for the sake of illustration, we describe the abovementioned setting procedure by specifically referring to the differential elements of a particular pair of DRs, namely that of DR_i and DR_j, which defines the respective DPZ_{ij}. Obviously, the proposed setting philosophy equally holds for every DPZ.

Despite the fact that communication between the DRs is obviously assumed, the associated delay (due to latency etc.) is negligible in distribution systems due to the short line lengths. Therefore, communication delay has no impact on the proposed protection scheme and it is omitted from the analysis presented below. It is further assumed that common supplementary functions included in commercial differential relays (e.g., harmonic-blocking) are enabled in this scheme.

A. Setting the Main Time-Delayed Current Differential Elements

1) Setting a Single Element

Assume that a percentage current differential element is enabled in DR_i and DR_j to protect the DPZ_{ij}. Such an element has the characteristic shown in Fig. 2. The operating current equals the magnitude of the vectorial sum of the currents measured by the CTs at both ends of DPZ_{ij} [refer to (1)], whereas the restraining current equals half the sum of the individual measured current magnitudes [refer to (2)]

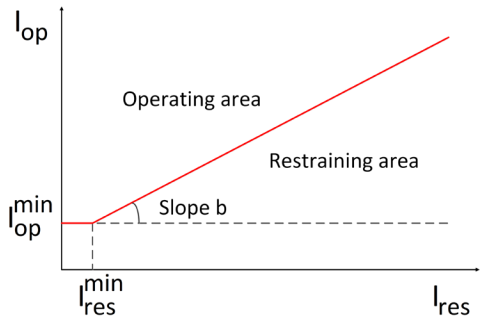

Fig. 2. Percentage differential characteristic.

Each DR trips its local circuit-breaker (CB) if (3) holds for a specified time delay $t_{d,ij}$:

$$I_{op,ij} = \left|\bar{I}_i + \bar{I}_j\right| \tag{1}$$

$$I_{res,ij} = \frac{\left|\bar{I}_i\right| + \left|\bar{I}_j\right|}{2} \tag{2}$$

$$I_{op,ij} > b_{ij} I_{res,ij} + I_{op,ij}^{\min} \tag{3}$$

$$t_{d,ij} \geq t_{p,ij} + t_{cti} \tag{4}$$

where b_{ij} is a bias factor defining the slope of the current differential characteristic, $I_{op,ij}^{\min}$ is the minimum pickup differential current threshold, $t_{p,ij}$ is the operating time of internal (lateral) MPDs or external (neighbor) DRs, and t_{cti} is the requested coordination time interval.

The slope b_{ij} is set to address several factors affecting the DRs performance and especially CT saturation. Larger bias factors limit the operating area and therefore they are preferred if protection security is of outmost concern. Indeed, protection security is preferred in this work and therefore, unless otherwise stated, the b setting value tends always to this direction.

$I_{res,ij}^{\min}$ is set to achieve adequate sensitivity, avoiding, however, an early trip which would compromise coordination. $I_{op,ij}^{\min}$ is set to avoid undesired trip under normal load/generation conditions, or external zone short-circuit faults. Hence, the appropriate setting of $I_{op,ij}^{\min}$ takes into account the current inequality at the two measurement points (CTs location) due to the lateral loads and the DG infeed, as well as external short-circuits causing the undesired operation of DPZ_{ij} especially under the DG infeed effect.

The appropriate choice of $t_{d,ij}$ depends on the specific protection objectives set to the DRs pair. For faults with a fault resistance up to a specified value (R_f^{sp}), occurring in the laterals of DPZ_{ij}, an intentional time delay $t_{d,ij}^{lat}$ must be selected to keep coordination between the DRs of this zone and its lateral MPDs. The respective differential element is set with a time-delay that is derived from the following criterion:

$$t_{d,ij}^{lat} \geq t_{mpd,ij}^{max} + t_{cti} \tag{5}$$

where $t_{mpd,ij}^{max}$ is the maximum MPD operating time resulted for all the common short-circuit fault types examined in the laterals of the DPZ_{ij}. If the MPD is a fuse, $t_{mpd,ij}^{max}$ corresponds to the maximum total clearing time $t_{tc,ij}^{max}$. Note that, in the latter case, a lower t_{cti} can be typically considered compared to the case where the MPD is an overcurrent relay. However, the same t_{cti} is always assumed in this paper, for the sake of simplicity.

If it is possible for DPZ_{ij} to detect external faults, another intentional time delay $t_{d,ij}^{ext}$ must be selected, for coordination with neighbor DPZs. For instance, if DPZ_{ij} and DPZ_{mn} are considered, the respective current differential element should also comply with the following condition:

$$t_{d,ij}^{ext} \geq t_{d,mn}^{lat} + t_{cti} \tag{6}$$

Ultimately, the largest time delay out of the two determined above is selected as the marginally required time delay setting $t_{d,ij}^{marg}$ of the DRs of interest:

$$t_{d,ij}^{\text{marg}} = \max\left\{t_{d,ij}^{\text{lat}}, t_{d,ij}^{\text{ext}}\right\} \quad (7)$$

2) Setting Multiple Elements

The time delay setting of (7) is appropriate to maintain coordination within a DPZ (for lateral faults) or between successive DPZs. However, at the same time, this time delay setting may be considered very high in case of faults occurring in the main feeder part covered by a DPZ. To deal with this problem, this paper proposes utilizing multiple time-delayed current differential elements instead of one in the DRs of each DPZ. These elements are accordingly graded with each other to operate in a coordinated manner. In this way, a better compromise between selectivity and DRs tripping time is achieved.

For setting multiple time-delayed current differential elements to protect the same DPZ (e.g. DPZ_{ij}), the following procedure is adopted. The minimum clearing time $t_{mpd,ij}^{\min}$ out of all clearing times of the MPDs inside the DPZ_{ij} is determined based on static short-circuit simulation analysis. The analysis examines short-circuit faults of any type, occurring at several places inside the DPZ_{ij}. Fault resistances up to the specified value R_f^{sp} are simulated. By adding the necessary coordination time interval t_{cti} to the minimum clearing time $t_{mpd,ij}^{\min}$, the conditionally fastest time-delay setting $t_{d,ij}^{\text{fast}}$ of the current differential elements is determined. The latter is given below:

$$t_{d,ij}^{\text{fast}} \geq t_{mpd,ij}^{\min} + t_{cti} \quad (8)$$

The next step is to calculate the time difference ($\Delta t_{d,ij}$) between the minimum required and the fastest possible time delay setting of the current differential elements in DPZ_{ij}:

$$\Delta t_{d,ij} = t_{d,ij}^{\text{marg}} - t_{d,ij}^{\text{fast}} \quad (9)$$

If a considerable time difference $\Delta t_{d,ij}$ comes out, then this time difference can be discretized by dividing it with a desired constant time period Δt_{des} (e.g. 100 ms). The rounded outcome plus one is the number of the multiple elements n to be set in DPZ_{ij}:

$$n = round\left(\frac{\Delta t_{d,ij}}{\Delta t_{des,ij}}\right) + 1 \quad (10)$$

In other words, n current differential elements will be set with the fastest having a time delay equal to $t_{d,ij}^{\text{fast}}$ and the slowest a time delay equal to $t_{d,ij}^{\text{marg}}$. The time delay of each intermediate current differential element k, enabled for DPZ_{ij}, will be:

$$t_{d,ij}^{\text{k}} = round\left(t_{d,ij}^{\text{fast}} + k\Delta t_{des}\right), \quad k = 1,\ldots,n-2 \quad (11)$$

After the determination of the number of current differential elements and their time-delay, the next step of the procedure is to set the pickup current threshold $I_{op,ij}^{\min\,(\text{k})}$ of each of those elements. This is a very important step since otherwise no discrimination between the multiple time-delayed current differential elements can be achieved. Note that the bias factor b_{ij} and the minimum restraining current $I_{res,ij}^{\min}$ are once decided for each current differential element, according to what is described in the previous subsection, and kept constant. Fig. 3 shows the flowchart of the above-described procedure.

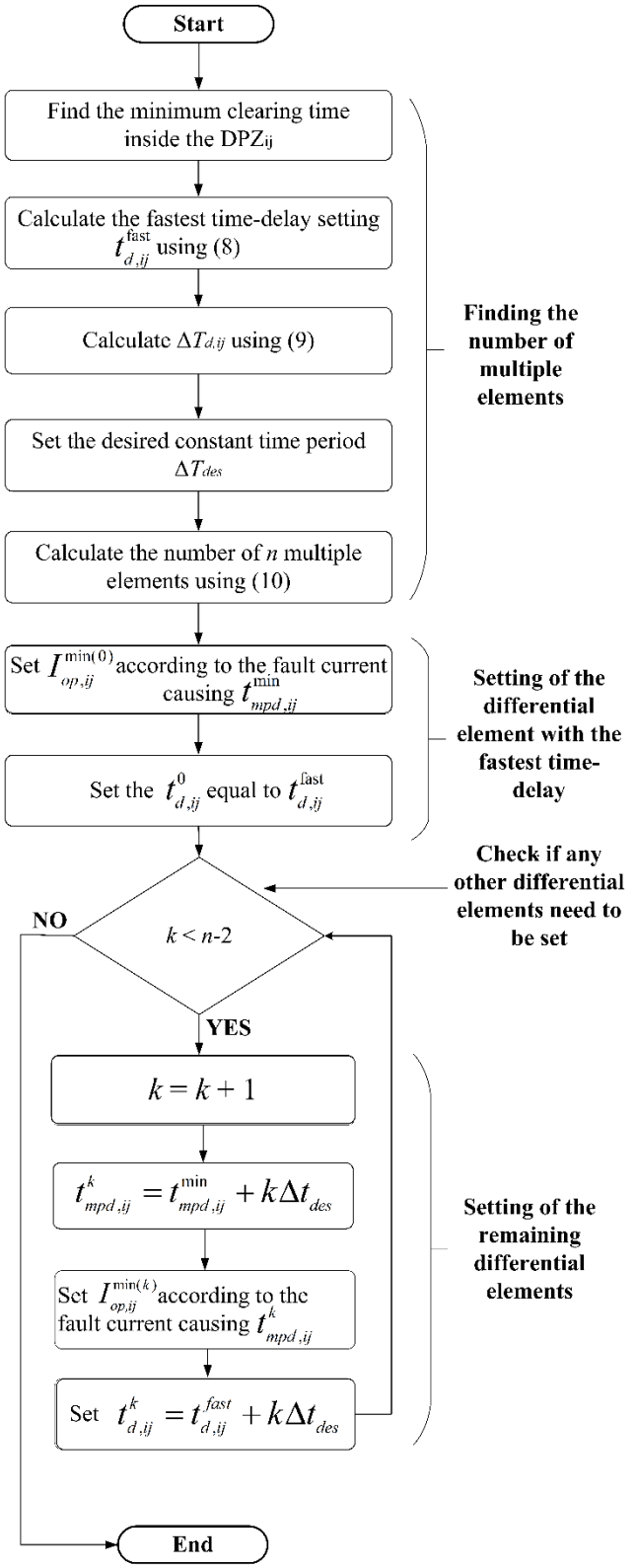

Fig. 3. Flowchart of multiple elements setting procedure.

Setting $I_{op,ij}^{\min\,(\text{k})}$ to each current differential element k aims at finding the short-circuit fault conditions that cause the slowest PD inside DPZ_{ij} to keep selectivity with the current differential element of interest. For instance, given the time delay $t_{d,ij}^{\text{k}}$ of element k (as derived based on the procedure described in Subsection III.A.1), the short-circuit fault magni-

tude, resistance and location causing the clearing time of the slowest PD to be marginally smaller than $t_{d,ij}^{k} - t_{cti}$ is sought.

B. Setting the Sensitive Time-Delayed Current Differential Element

In order to deal with relatively high impedance faults exclusively, an additional time-delayed current differential element is enabled in each DRs pair. This element has a more sensitive characteristic, intending to efficiently protect against faults with fault resistance at least up to 40 Ω (or greater), regardless of whether coordination between the DRs and the zone's PDs is preserved or not. Note that the 40 Ω resistance is a typical maximum fault resistance value considered in actual protection design studies [32].

The pick-up differential current threshold $I_{op}^{\min}$ of this element is set slightly higher than the maximum differential current expected during normal system operation, considering all the possible system states. Focusing again on DR_i and DR_j, the above criterion is described as below:

$$I_{op,ij}^{\min} > c_{ij} I_{diff,ij}^{\max} \quad (12)$$

where $I_{diff,ij}^{\max}$ is the maximum differential current sensed by DR_i and DR_j under all the possible normal system pre-fault conditions, and c_{ij} is a security factor.

In order to avoid overlaps, the sensitive current differential element should be set with a time delay $t_{d,ij}$ which is greater than the $t_{d,ij}^{\min}$ set to preserve coordination with the MPDs within the DPZ_{ij} as well as with successive DPZs (see previous subsection). If this leads to an unacceptable time delay setting, that is to a time delay setting exceeding the through-fault damage time limitation of any of the zone's equipment, then the time-delay setting of the sensitive current differential element will be restricted to the acceptable upper time limit (t_{utl}) imposed by this limitation:

$$t_{utl} \geq t_{d,ij} > t_{d,ij}^{\min} \quad (13)$$

It is noted that $I_{res,ij}^{min}$ can be set as high as required to achieve the desired sensitivity, since there is no danger of compromising coordination in that case.

C. Setting the Instantaneous Current Differential Element

It is understood that it is preferrable to clear short-circuit faults occurring at the main feeder line part of a DPZ instantaneously. However, as addressed in Subsection III.B, this is difficult to achieve due to the need of coordination with the lateral PDs. Indeed, a fault at the beginning of a lateral (i.e. F_A in Fig. 1) practically produces almost the same fault current magnitude with that of a fault (i.e. F_B in Fig. 1) in the main line close to this lateral. Hence, discrimination is not possible and instantaneous elements cannot be applied.

However, for short-circuit faults occurring at the main feeder line and up to the connection point of the first lateral within the zone (e.g. F_C in Fig. 1), an instantaneous current differential element can be enabled in the DRs pair. The respective differential current elements are set with no intentional time-delay:

$$t_{d,ij} \simeq 0 \quad (14)$$

Fig. 4 indicatively illustrates the respective differential element characteristic. It is noteworthy that $I_{res,ij}^{min}$ could probably be freely set as high as required in that case, since the instantaneous characteristic will expectedly be placed safely above the rest differential characteristics.

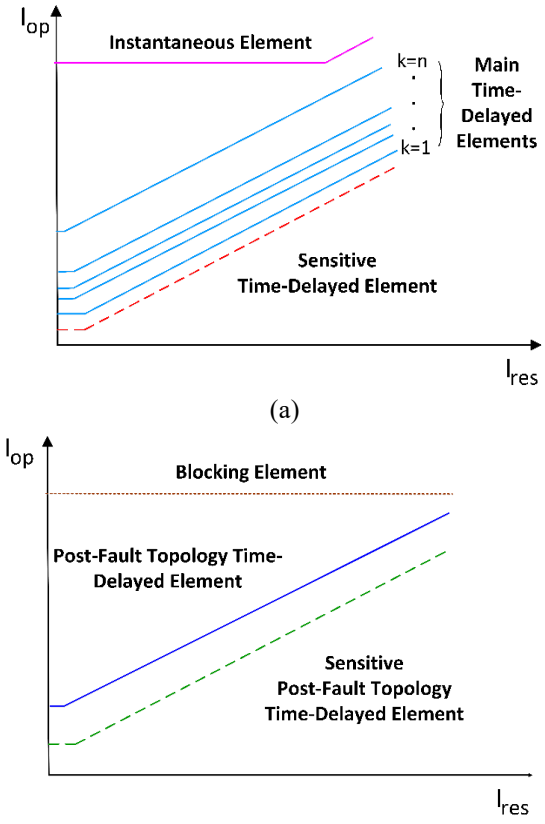

Fig. 4. Multi-element characteristics of a DR. (a) Elements enabled during pre-fault conditions, (b) Elements enabled during post-fault conditions.

IV. Protection Scheme for Emergency Conditions

A. Breaker-Failure Protection

For the case where a CB fails to open, although a trip order has been issued by the respective DR, a breaker-failure (BF) scheme is additionally designed to enhance protection security. The latter ensures that if a CB fails to open after receiving a trip signal by its corresponding DR, an alternative CB will be tripped by the same DR to clear the fault. For instance, referring to Fig. 1, if a fault occurs in the DPZ_{ij}, the CBs (not explicitly shown in Fig. 1) at the location of DR_i and DR_j should be tripped by these relays. Assume now that CB_i (i.e. the CB controlled by DR_i) trips correctly but CB_j (i.e. the CB controlled by DR_j) fails to open. Then, DR_j will trip another CB, which in this example will be the CB_m (or CB_n if DR_j and DR_m share the same CB_m in a less expensive implementation).

Fig. 5 shows the designed BF trip logic of DR_j. Once DR_j issues a trip order to CB_j, a BF initiation (BFI) signal is simultaneously asserted. We assume that BFI signal remains active for a proper time duration. Afterwards, the state of CB_j is checked for a time period equal to t_{BF}. Typically, t_{BF} lasts for 7-15 cycles [33], to compensate for the CB_j interrupting time

plus any other delays associated with the relay. If CB_j remains closed after t_{BF} expires, DR_j trips the alternative CBs. In the meantime, a re-trip command is issued to CB_j, as a second attempt to trip this CB, in order to avoid opening remote CBs. The re-trip time delay (t_{RT}) is set to 1-2 cycles, just to avoid misoperation due to nuisance input (e.g. noise) [33].

It is further assumed that common supplementary functions included in commercial differential relays (e.g., harmonic-blocking) are enabled in this scheme.

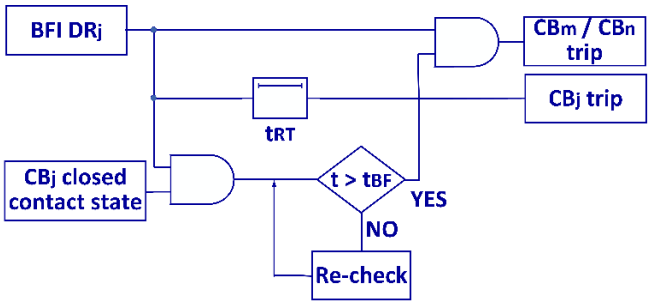

Fig. 5. Breaker-failure trip logic of a DRi.

B. Post-Fault Topology Protection

When a DR pair trips correctly, a part of the distribution system is disconnected. For such a change in network topology, the differential current measured by the remaining DRs during the post-fault system operation may change significantly. Hence, the settings resulting from the methodology of the previous section, which are calculated taking into consideration the pre-fault network topology, may not be suitable under the new system conditions.

To cope with this problem, the post-fault topology time-delayed current differential element is introduced. This element is beforehand set in each DR pair and is enabled only if any other differential element in the system has previously tripped, causing a subsequent topology change.

The post-fault topology protection element enables a single current differential characteristic (Fig. 4b), which replaces all the previous ones (i.e. the multiple time-delayed, sensitive, and instantaneous characteristics). It is set to detect all the internal faults with a fault resistance up to R_f^{sp}, retaining the protection coordination logic with the lateral PDs in the post-fault system state. For this purpose, proper time delay (t_d) and pickup differential current threshold settings ($I_{pf,op}^{min}$, $I_{pf,res}^{min}$) are determined, based on a detailed simulation-based setting procedure. The latter examines all the critical faults and the different network operation states.

If faults with higher resistance than R_f^{sp} are to be cleared, then a second sensitive post-fault topology protection element can be set (also shown in Fig. 4b). Again, proper settings must be determined for the pickup differential current threshold $I_{spf,op}^{min}$, the restraining current $I_{spf,res}^{min}$, and the time delay t_d of this sensitive differential element through simulations.

It is noted that a limited number of current differential characteristics is enabled in this case, resulting in safe-side but non-optimal operation times. This is for protection scheme design simplicity, given that the post-fault topology regards a temporary and emergency situation. A more detailed configuration could optionally be set, by following the methodology proposed previously for the main topology.

Although the post-fault topology current differential elements provide the required protection sensitivity, they raise some selectivity issues in ring-type networks. For instance, a very sensitive setting may cause a false DR trip for an external fault (i.e. in the nearby DPZ). Such a nuisance trip may occur due to the change from a ring to a radial network topology, which leads to only one CT taking current measurements in some DPZs (i.e. those which are not fed by a downstream DG unit, but include DG). Nevertheless, this problem can be overcome by sending a blocking signal to neighboring DRs, if a fault is certainly recognized inside a specific DPZ.

For this purpose, an independent differential current threshold I_{pf}^{bl} is defined in each DRs pair, enabled as long as the post-fault topology is maintained. In fact, this is the minimum differential current seen by the DRs during an internal fault, that concurrently causes a false trip of nearby DPZs. If the measured differential current exceeds this threshold, a blocking signal is sent to the DRs of a neighboring DPZ. Note that this threshold results after a detailed offline fault-simulation study, while it is ensured that it is not exceeded in more than one DPZs at the same time (i.e. it is exceeded only in the faulted DPZ).

Note that the activation of the normal/sensitive post-fault topology time-delayed elements, as well as the activation of the blocking element, are triggered by a pilot signal sent from the tripped DRs to all other DRs. In other words, when a trip command is asserted in any DR, a setting group change command is sent to all other DRs in the distribution system to disable the normal topology elements (Fig. 4a) and enable the post-fault topology elements (Fig. 4b). It is obvious that for this purpose, the DRs should communicate with each other and have two setting groups beforehand stored in their memory: one setting group for the normal system topology and a second for the post-fault system topology. Since these complimentary setting groups provide adequate network protection for the normal and the post-fault topology respectively and are enabled when a change in the network topology occurs, the proposed protection scheme can be characterized as an adaptive protection solution supported by communications means.

V. Application Study

A. Examined Power Distribution System

The proposed protection scheme is tested through simulations in the real power distribution system model depicted in Fig. 6. PowerFactory software is used for the simulations. The examined test system is formed by two 20-kV, mixed overhead (OH)-underground (UG) distribution feeders of the city of Xanthi, Greece, namely Line-23 and Line-24. Each feeder is assumed hosting one 3-MW-rated photovoltaic (PV) unit (with a maximum steady-state short-circuit current of 1 p.u.) and two 1.5-MW-rated synchronous generators (SGs). The laterals of the overhead line part, as well as the distribution transformers spread along the network, are protected by a fuse

installed at their departure and their primary side, respectively. Further technical details of this system can be found in [34].

Due to the different line characteristics and configuration of the overhead network compared to the underground one, the present analysis is performed separately for these line parts. Based on that, a single DPZ is formed to protect the entire overhead line part of each feeder, and two other DPZs are responsible to protect the underground part. All these zones are shown in Fig. 6 with different line styles and colors.

B. Simulation Methodology

The setting procedure comprises an extensive simulation study, which is conducted considering the following system conditions:

- Minimum and maximum system load conditions, that is 40%S_{total} and 100%S_{total}, respectively; S_{total} (15.93 MVA) is the maximum simultaneously expected load consumption on both feeders (Line-23 and Line-24) when the network is operated as a ring.
- Minimum and maximum DG penetration, that is 0 and 75%S_{total}, respectively.

The bias factor b is set equal to 80% in all the DRs for increased protection security. Safety factor c is taken equal to 1.1, whereas Δt_{des} is assumed equal to 100 ms.

Table I includes the time data of the DRs constituting each DPZ formed, resulting from the methodology proposed in Subsection III. First of all, the maximum and minimum total clearing time ($t_{tc}^{\max}$ and $t_{tc}^{\min}$, respectively) of the main lateral fuse inside each DPZ is calculated, by conducting all the types of fault at multiple lateral points, considering all the marginal fault/system conditions. By adding a typical t_{cti} of 0.3 s, we determine the minimum required and fastest time delay setting ($t_d^{\min}$ and t_d^{fast}, respectively) of a differential element enabled in each DPZ. Then, by using (10), we calculate the total number of differential elements that have to be enabled in each DPZ, to achieve the proposed multi-element coordinated operation (refer to the Δt_d and n values of Table I).

The complete settings of the DRs in each DPZ are presented in Table II. As for $DPZ_{1,1'}$ and $DPZ_{5,5'}$, the time delay setting t_d of the intermediate differential elements between the slowest and the fastest one (as determined in Table I), is calculated using (11). The $I_{op}^{\min}$ and $I_{res}^{\min}$ setting of each differential element of a DPZ is set based on a detailed simulation study (refer to Subsection III.A), ensuring that, under any fault/system conditions, a fault detected by this element will not result in miscoordination between the corresponding DRs and a fuse inside this DPZ. It is noted that, due to intermediate DG infeed, a differential element of a DPZ can also detect faults occurring in an adjacent DPZ; however, proper check is made to ensure that the time delay setting of such an element is safely above the time delay setting of the tripping element of the faulted DPZ.

Table II also includes the resulting settings of the sensitive and the instantaneous current differential elements. For setting the $I_{op}^{\min}$ and $I_{res}^{\min}$ of the sensitive elements, a detailed load-flow simulation study is conducted, ensuring that undesired tripping of these elements is avoided under normal system conditions (refer to Subsection III.B). The time delay of these elements is set to 2 s, which is the upper time limit (t_{utl}) imposed by the damage curve of the main substation transformer. Obviously, this time delay setting is high enough to coordinate with the rest differential elements of the same DPZ.

The instantaneous elements are set with no intentional time delay, while their $I_{op}^{\min}$ and $I_{res}^{\min}$ are set to allow tripping only for severe faults occurring in the first main line segment, i.e., before the first lateral of each DPZ (refer to Subsection III.C). Since such a main line segment is absent from $DPZ_{3,3'}$, an instantaneous element is not enabled for this zone.

The representative case of $DPZ_{1,1'}$ is chosen in Fig. 7, to illustrate the resulting differential characteristics.

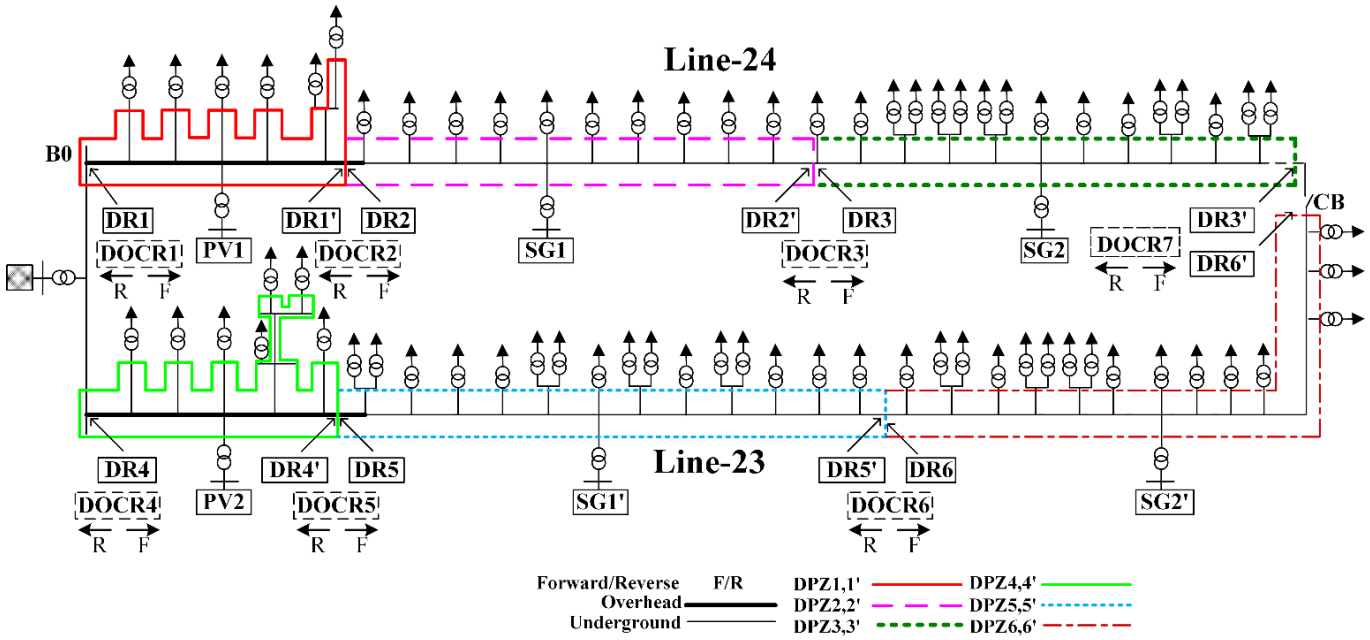

Fig. 6. Examined distribution system.

Table III shows the resulting settings for the post-fault topology protection elements. Since the network topology change from ring to radial can now more easily result in false tripping of a differential element due to an external fault (refer to Subsection IV.B), setting I_{pf}^{bl} is crucial.

TABLE I
DETERMINING TIME DATA AND NUMBER OF MAIN DIFFERENTIAL ELEMENTS

DPZ	$t_{tc}^{\max}$ (ms)	$t_{tc}^{\min}$ (ms)	$t_d^{\min}$ (ms)	t_d^{fast} (ms)	Δt_d (ms)	n
1,1′	405	14	705	314	391	5
2,2′	138	14	438	314	124	2
3,3′	141	14	441	314	131	2
4,4′	408	14	708	314	396	5
5,5′	65	13	365	313	52	2
6,6′	68	13	368	313	57	2

TABLE II
RESULTING SETTINGS OF THE DIFFERENTIAL ELEMENTS OF EACH DPZ

DPZ	Differential element	$I_{op}^{\min}$ (A pri)	$I_{res}^{\min}$ (A pri)	t_d (ms)
1,1′	1	276	162	705
	2	352	40	600
	3	452	40	500
	4	668	40	400
	5	2944	40	314
	Sensitive	128	288	2000
	Instantaneous	6816	3408	0
2,2′	1	288	30	438
	2	1512	20	314
	Sensitive	100	45	2000
	Instantaneous	5596	2823	0
3,3′	1	318	20	441
	2	1528	20	314
	Sensitive	160	80	2000
	Instantaneous	N/A	N/A	N/A
4,4′	1	272	152	708
	2	348	40	600
	3	444	40	500
	4	656	40	400
	5	2940	40	314
	Sensitive	120	296	2000
	Instantaneous	6552	3277	0
5,5′	1	288	30	365
	2	978	30	313
	Sensitive	114	65	2000
	Instantaneous	5442	2756	0
6,6′	1	310	20	368
	2	980	20	313
	Sensitive	116	60	2000
	Instantaneous	5162	2610	0

TABLE III
RESULTING SETTINGS OF THE POST-FAULT TOPOLOGY DIFFERENTIAL ELEMENTS OF EACH DPZ

EDPZ	Differential element	$I_{op}^{\min}$ (A pri)	$I_{res}^{\min}$ (A pri)	I_{pf}^{bl} (A pri)	t_d (ms)
1,1′	Main	300	452	1441	715
	Sensitive	132	457	N/A	2000
2,2′	Main	462	514	2818	525
	Sensitive	106	283	N/A	2000
3,3′	Main	492	424	2665	495
	Sensitive	165	193	N/A	2000
4,4′	Main	288	429	1323	725
	Sensitive	140	474	N/A	2000
5,5′	Main	456	483	3392	405
	Sensitive	121	277	N/A	2000
6,6′	Main	448	387	2165	405
	Sensitive	121	187	N/A	2000

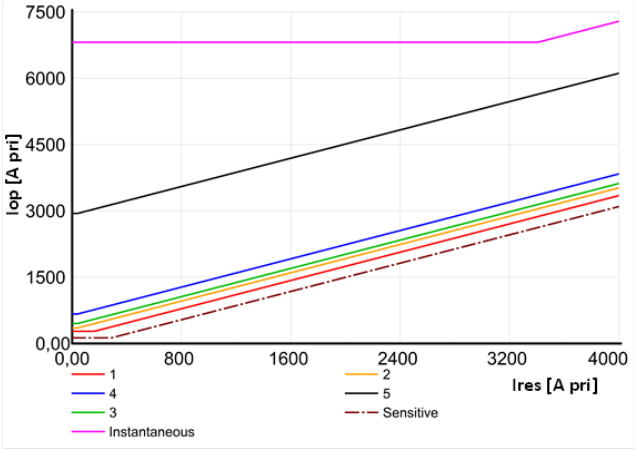

Fig. 7. Differential element characteristics of DPZ$_{1,1'}$.

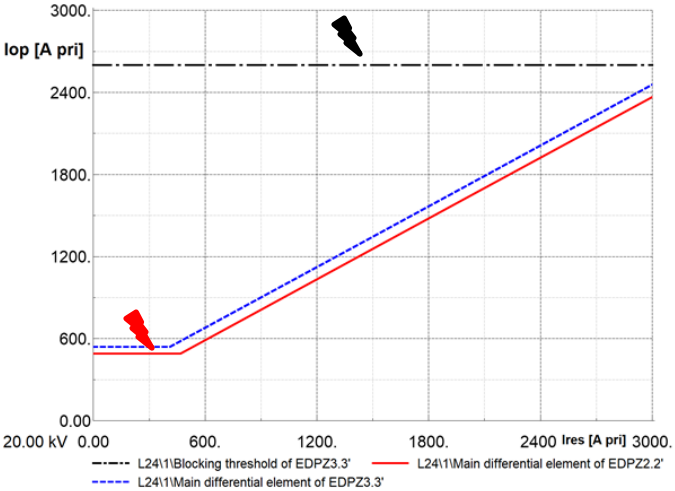

Fig. 8. Setting the blocking current differential threshold for DPZ$_{3,3'}$.

Fig. 8 provides an example of setting I_{pf}^{bl} for the post-fault differential element of DPZ$_{3,3'}$, considering the marginal fault scenario for this specific case (i.e., a LG fault inside DPZ$_{3,3'}$). As shown, the simulated fault is detected inside the operating area of the main element of interest (i.e., that of DPZ$_{3,3'}$), as well as the operating area of the respective element enabled for the adjacent DPZ$_{2,2'}$. This could normally lead to undesired double tripping, as there is a very small difference between the time delay of the two elements (refer to Table III).

In order to avoid considerably increasing the time delay of the main post-fault topology element of DPZ$_{2,2'}$ for this purpose, I_{pf}^{bl} is properly set for EDPZ$_{3,3'}$ (corresponding to the horizontal dotted line of Fig. 8), so that a blocking signal is sent by the element of DPZ$_{3,3'}$ to that of DPZ$_{2,2'}$, once the I_{op} calculated by the former exceeds this threshold. Of course, this setting is chosen to be suitable for any possible fault that would cause concurrent tripping of an adjacent DPZ.

Finally, besides the static fault simulation study required to set the examined DRs, the performance of the designed protection scheme has been successfully tested via time-domain fault simulations. Due to space limitation, two representative examples are illustrated in Fig. 9a and Fig. 9b.

Fig. 9a regards a 10-Ω LG fault, occurring at the endpoint of lateral L$_4$′, at t = 1 s. This lateral is primarily protected by a

fuse at its departure, and secondarily by $DPZ_{4,4'}$. As shown, the fault is cleared by the lateral fuse after approximately 0.35 s. During the fault, the first differential element of $DPZ_{4,4'}$ also picks up; however, since it is delayed by 0.708 s, it does not trip, coordinating with the lateral fuse.

Fig. 9b concerns a solid LLL fault, occurring in the main line part primarily protected by $DPZ_{2,2'}$ (i.e., at bus B_{12}). The fault is detected by the second differential element of this zone, which trips after 0.314 s and clears the fault. It is worth mentioning that, if the conventional setting approach (e.g. as in [31]) was followed, instead of the proposed multi-element approach, the fault would be cleared after 0.438 s, as practically only the first differential element would be enabled. It is also noted that, as shown in Fig. 9b, the I_{op} measured during the fault is suddenly decreased 0.16 s after fault inception; this due to the disconnection of DG units by undervoltage interconnection protection. However, the DRs of $DPZ_{2,2'}$ operate correctly, further proving the immunity of the proposed setting methodology to DG intermittence.

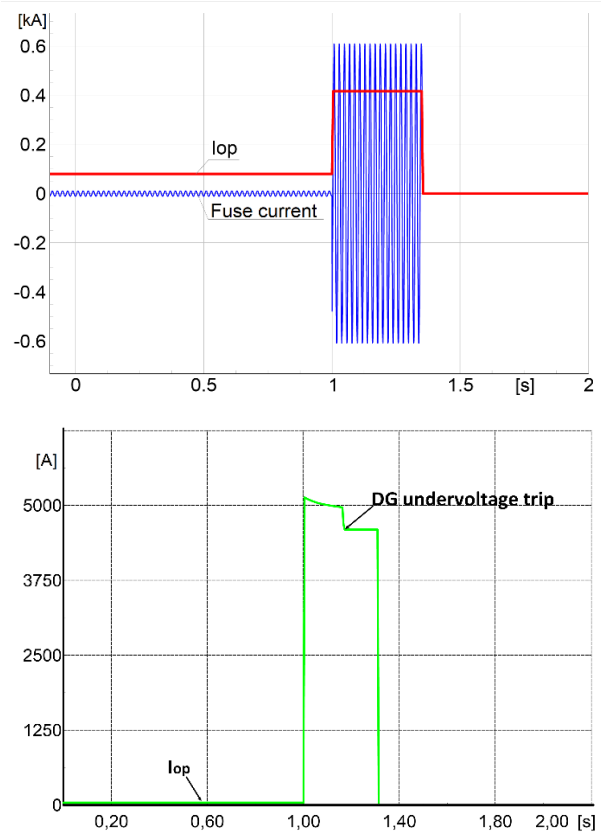

Fig. 9. (a) Current through lateral fuse and differential current of $DPZ_{4,4'}$. (b) Differential current of $DPZ_{2,2'}$.

C. Comparison with Directional Overcurrent Protection

In this section the proposed differential protection scheme is compared with a typical directional overcurrent protection scheme. For this purpose, directional overcurrent relays (DOCRs) are assumed at each place where DRs are installed in the test distribution system of Fig. 6. Each DOCR (shown with a dashed line in Fig. 6) is a dual-setting device with a specific setting group against forward (F) and reverse (R) faults.

A detailed short-circuit study is conducted to determine the necessary DOCR settings for each direction. In this case, selectivity means that each DOCR must be coordinated with all the successive DOCRs as well as with the slowest fuse in a specific direction (forward or reverse). The study investigates all common solid/non-solid fault types (i.e., single-phase-ground, double-phase, double-phase-ground, three-phase) along the feeders (Line-23 and Line-24). Note that the IEC very inverse curve has been chosen for the DOCRs since it fits better to most of the fuse characteristics (not shown here).

Figure 10 depicts a representative coordination example, where the tripping time of the phase elements of three successive DOCRs (i.e., DOCR1, DOCR2, and DOCR3) for a three-phase fault (LLL) at the remotest end of Line-24 is shown. Assuming a CTI equal to 0.3 s, one can see that the three DOCRs will trip in a coordinated manner. Table IV presents the tripping time of DRs and DOCRs for some indicative fault scenarios examined in the comparative study. As it can be seen, the DRs give (in most cases) a faster tripping time compared to the DOCRs for the same fault type, fault resistance, and fault position.

Note, however, that the need of a voltage transformer to be installed together with the CT and the DOCR increases the cost of the directional overcurrent scheme, whereas the difficulty to find a unique setting for the single phase/ground directional element in order to effectively deal with all faults (especially those involving fault resistance) occurring in an active distribution system (like that shown in Fig. 6) makes this standard methodology challenging from the very beginning.

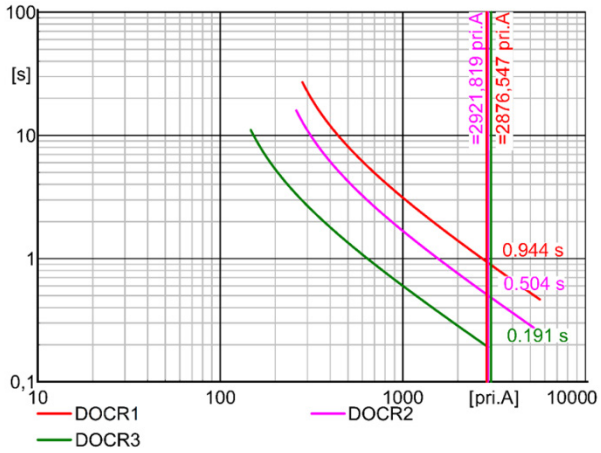

Fig. 10. LLL forward fault in front of DOCR3.

TABLE IV
COMPARISON OF TRIPPING TIMES OF DRS AND DOCRS

Acting device	Fault in the middle of DPZ			Fault in front of slowest fuse		
	LLL (0Ω)	LG (5Ω)	LG (8Ω)	LLL (0Ω)	LG (5Ω)	LG (8Ω)
Tripping time of DRs (s)						
DPZ1	0.314	0.400	0.400	0.314	0.400	0.500
DPZ2	0.314	0.438	0.438	0.314	0.438	0.438
DPZ3	0.314	0.441	0.441	0.314	0.441	0.441
Tripping time of DOCRs (s) for above fault locations						
DOCR1,2	0.502	1.582	2.786	0.525	1.796	3.062
DOCR2,3	0.312	0.476	0.510	0.350	0.476	0.578
DOCR3,7	0.219	0.206	0.206	0.191	0.206	0.206

VI. Conclusion

This paper introduces a multi-element line differential protection approach, suitable for DG-integrated distribution systems. Unlike existing differential protection schemes, this approach applies multiple differential elements to each DPZ, forming a time-graded scheme for effective coordination with lateral protection. A sensitive and an instantaneous differential element is also enabled in each DPZ, against high-impedance and severe faults, respectively. An adaptive approach is proposed to ensure protection reliability after a DPZ trips. A blocking-based logic is applied in this case, to avoid nuisance tripping of a zone during external faults, caused by DG infeed. Dealing with this kind of nuisance tripping constitutes another contribution of this work. A BF protection scheme is further designed for backup protection.

The applicability of the proposed DR setting methodology is proven on a real distribution system with DG, considered operating in a ring configuration. The enhanced performance of the designed protection scheme is demonstrated via time-domain fault simulations, which show the superiority of the proposed approach compared to the conventional one.

VII. References

[1] M. H. J. Bollen, F. Hassan, *Integration of Distributed Generation in the Power System*. Hoboken, NJ, USA: Wiley-IEEE Press, 2011.

[2] S. T. P. Srinivas, P. P. Verma, K. S. Swarup, "A novel convexified linear program for coordination of directional overcurrent relays," *IEEE Trans. Power Del*., vol. 34, no. 2, pp. 769-772, Apr. 2019.

[3] E. Purwar, D. N. Vishwakarma, S. P. Singh, "A novel constraints reduction based optimal relay coordination method considering variable operational status of distribution system with DGs," *IEEE Trans. Smart Grid*, vol. 10, no.1, pp. 889-898, Jan. 2019.

[4] R. Jain, D. L. Lubkeman, S. M. Lukic, "Dynamic adaptive protection for distribution systems in grid-connected and islanded modes," *IEEE Trans. Power Del*., vol. 34, no. 1, pp. 281-289, Feb. 2019.

[5] M. Ojaghi, V. Mohammadi, "Use of clustering to reduce the number of different setting groups for adaptive coordination of overcurrent relays," *IEEE Transactions Power Del*., vol. 33, no. 3, pp. 1204-1212, Jun. 2018.

[6] H. M. Sharaf, H. H. Zeineldin, E. El-Saadany, "Protection coordination for microgrids with grid-connected and islanded capabilities using communication assisted dual setting directional overcurrent relays," *IEEE Trans. Smart Grid*, vol. 9, no. 1, pp. 143-151, Jan. 2018.

[7] Z. Zhang, B. Xu, P. Crossley, L. Li, "Positive-sequence-fault-component-based blocking pilot protection for closed-loop distribution network with underground cable," *Int. J. Elect. Power Energy Syst*., vol. 94, pp. 57-66, Jan. 2018.

[8] J. J. Q. Yu, Y. Hou, A. Y. S. Lam, V. O. K. Li, "Intelligent fault detection scheme for microgrids with wavelet-based deep neural networks," *IEEE Trans. Smart Grid*, vol. 10, no. 2, pp. 1694-1703, Mar. 2019.

[9] S. Choi, A. P. S. Meliopoulos, "Effective real-time operation and protection scheme of microgrids using distributed dynamic state estimation," *IEEE Transactions Power Del*., vol. 32, no. 1, pp. 504-514, Feb. 2017.

[10] A. M. Tsimtsios, V. C. Nikolaidis, "Towards plug-and-play protection for meshed distribution systems with DG," *IEEE Trans. Smart Grid*, vol. 11, no. 3, pp. 1980-1995, May 2020.

[11] K. Pandakov, C. M. Adrah, H. K. Høidalen, Ø. Kure, "Experimental validation of a new impedance-based protection for networks with distributed generation using co-simulation test platform," *IEEE Transactions Power Del*., vol. 35, no. 3, pp. 1136-1145, Jun. 2020.

[12] M. Elkhatib, A. Ellis, "Communication-assisted impedance-based microgrid protection scheme," in *Proc. IEEE Power & Energy Soc. General Meeting*, Chicago, IL, USA, Jul. 16-20, 2017, pp. 1-5.

[13] A. M. Tsimtsios, G. N. Korres, V. C. Nikolaidis, "A pilot-based distance protection scheme for meshed distribution systems with distributed generation," *Int. J. Elect. Power Energy Syst*., vol. 05, pp. 454-469, Feb. 2019.

[14] T. S. Ustun,, R. H. Khan, "Multiterminal hybrid protection of microgrids over wireless communications network," *IEEE Trans. Smart Grid*, vol. 6, no. 5, pp. 2493-2500, Sep. 2015.

[15] W. Li, Y. Tan, Y. Li, Y. Cao, C. Chen, M. Zhang, "A new differential backup protection strategy for smart distribution networks: A fast and reliable approach," *IEEE Access*, vol. 7, pp. 38135-38145, Mar. 2019.

[16] X. Li and Y. Lu, "Improved amplitude differential protection scheme based on the frequency spectrum index for distribution networks with DFIG-based wind DGs," *IEEE Access*, vol. 8, pp. 64225-64237, Mar. 2020.

[17] A. C. Adewole, A. D. Rajapakse, D. Ouellette, and P. Forsyth, "Protection of active distribution networks incorporating microgrids with multi-technology distributed energy resources," *Electric Power Syst. Res.*, to be published.

[18] C. D. Prasad, M. Biswal, and A. Y. Abdelaziz, "Adaptive differential protection scheme for wind farm integrated power network," *Electric Power Syst. Res.*, to be published.

[19] L. Zang, G. Zou, C. Zhou, L. Sun and X. Du, "A current differential protection scheme based on Q-axis component for distribution networks," in *Proc. 6th Asia Conf. Power Elect. Eng. (ACPEE)*, Chongqing, China, Apr. 8-11, 2021, pp. 24-28.

[20] K. A. Wheeler, S. O. Faried, and M. Elsamahy, "A microgrid protection scheme using differential and adaptive overcurrent relays," in *Proc. IEEE Elect. Power Energy Conf. (EPEC)*, Saskatoon, SK, Canada, Oct. 22-25, 2017, pp. 1-6.

[21] H. Gao, J. Li, B. Xu, "Principle and implementation of current differential protection in distribution networks with high penetration of DGs," *IEEE Transactions Power Del*., vol. 32, no. 1, pp. 565-574, Feb. 2017.

[22] B. Han, H. Li, G. Wang, D. Zeng, Y. Liang, "A virtual multi-terminal current differential protection scheme for distribution networks with inverter-interfaced distributed generators," *IEEE Trans. Smart Grid*, vol. 9, no. 5, pp. 5418-5431, Sep. 2018.

[23] H. Li, C. Deng, Z. Zhang, Y. Liang, G. Wang, "An adaptive fault-component-based current differential protection scheme for distribution networks with inverter-based distributed generators," *Int. J. Elect. Power Energy Syst*., to be published.

[24] B. Han, G. Wang, H. Li, and D. Zeng, "An improved pilot protection for distribution network with inverter-interfaced distributed generations," in *Proc. IEEE PES Asia-Pacific Power Energy Eng. Conf. (APPEEC)*, Xi'an, China, Oct. 25-28, 2016, pp. 2555-2559.

[25] E. Sortomme, S. S. Venkata, J. Mitra, "Microgrid protection using communication-assisted digital relays," *IEEE Transactions Power Del*., vol. 25, no. 4, pp. 2789-2796, Oct. 2010.

[26] C. Yuan, K. Lai, M. S. Illindala, M. A. Hajahmed, A. S. Khalsa, "Multi-layered protection strategy for developing community microgrids in village distribution systems," *IEEE Transactions Power Del.*, vol. 32, no. 1, pp. 495-503, Feb. 2017.

[27] X. Liu, M. Shahidehpour, Z. Li, X. Liu, Y. Cao, W. Tian, "Protection scheme for loop-based microgrids," *IEEE Trans. Smart Grid*, vol. 8, no. 3, pp. 1340-1349, May 2017.

[28] A. Thirumalai, X. Liu, and G. G. Karady, "Ultra fast pilot protection of a looped distribution system," in *Proc. IEEE PowerTech*, Trondheim, Norway, Jun. 19-23, 2011, pp. 1-8.

[29] C. Luo, J. Yang, Y. Sun, M. Cai, J. Wu, and L. Xu, "A network based protection scheme of distribution system," in *Proc. IEEE Int. Conf. Power Syst. Technol. (POWERCON)*, Auckland, New Zealand, Oct. 30-Nov. 2, 2012, pp. 1-6.

[30] T. S. Aghdam, H. K. Karegar, H. H. Zeineldin, "Variable tripping time differential protection for microgrids considering DG stability," *IEEE Trans. Smart Grid*, vol. 10, no. 3, pp. 2407-2415, May 2019.

[31] V.C. Nikolaidis, G. Michaloudis, A.M. Tsimtsios, D. Tzelepis, C.D. Booth, "A multi-zone differential protection scheme for MV distribution systems with distributed generation," in *Proc.15th Int. Conf. Develop. Power Syst. Protection (DPSP 2020)*, Liverpool, UK, Mar. 9-12, 2020, pp. 1-6.

[32] L. L. Grigsby, *Electric Power Generation, Transmission and Distribution*. Boca Raton, FL, USA: CRC Press, 2012.

[33] Y. Xue, M. Thakhar, J. C. Theron, D. P. Erwin, "Review of the breaker failure protection practices in utilities," in *Proc. 65th Annu. Conf. Protective Relay Engineers*, College Station, TX, USA, Apr. 2-5, 2012, pp. 260-268.

[34] A. M. Tsimtsios, V. C. Nikolaidis, "Application of distance protection in mixed overhead-underground distribution feeders with distributed generation," *J. Eng*., vol. 2018, no. 15, pp. 950-955, Oct. 2018.

VIII. Biographies

Vassilis C. Nikolaidis (M' 2011, SM' 2018) received the five-year Diploma of Electrical and Computer Engineering from the Department of Electrical and Computer Engineering, Democritus University of Thrace, Xanthi, Greece, in 2001, the M.Eng. degree in Energy Engineering and Management from National Technical University of Athens (NTUA), Athens, Greece, in 2002, and the Doctor of Engineering from NTUA, in 2007. Since 2008 he has been working as a power systems consulting engineer. Currently he is an Assistant Professor in the Department of Electrical and Computer Engineering, Democritus University of Thrace, Greece. His research interests mainly deal with power system protection, control, stability, and transients.

George Michaloudis received the Diploma and M.Eng. degree in Electrical and Computer Engineering from the Department of Electrical and Computer Engineering, Democritus University of Thrace, Xanthi, Greece, in 2018 and 2020, respectively. His research interests deal with power system protection.

Aristotelis M. Tsimtsios (S'17, M' 2021) received the Diploma of Electrical and Computer Engineering, the M.Sc. in Energy Systems and Renewable Energy Sources and the Ph.D. in Power System Protection from the Department of Electrical and Computer Engineering, Democritus University of Thrace, Xanthi, Greece, in 2013, 2015 and 2020, respectively. Since 2020, he has been with PROTASIS SA, as a power systems engineer. His research interests include power system protection and distributed generation.

Dimitrios Tzelepis (S'13–M'17) received the B.Eng. degree (Hons.) in electrical engineering from the Technological Education Institution of Athens, Athens, Greece, in 2013, and the M.Sc. degree in wind energy systems and the Ph.D. degree from the University of Strathclyde, Glasgow, U.K., in 2014 and 2017, respectively. He is currently a Research Fellow with the Department of Electronic and Electrical Engineering, University of Strathclyde. His research interests include power system protection, automation and control of future electricity grids, incorporating increased penetration of renewable energy sources, and high voltage direct current interconnections. His main research methods include implementation of intelligent algorithms for protection, fault location and control applications, including the utilization of machine learning methods and advanced and intelligent signal processing techniques.

Campbell D. Booth received the B.Eng. and Ph.D. degrees in electrical and electronic engineering from the University of Strathclyde, Glasgow, U.K., in 1991 and 1996, respectively. He is currently a Professor and the Head of the Department for Electronic and Electrical Engineering, University of Strathclyde. His research interests include power system protection, plant condition monitoring and intelligent asset management, applications of intelligent syatem techniques to power system monitoring, protection, and control, knowledge management, and decision.